World Journal of Advanced Engineering Technology and Sciences
eISSN: 2582-8266
Cross Ref DOI: 10.30574/wjaets
Journal homepage: https://wjaets.com/

(RESEARCH ARTICLE)

Check for updates

Robust Multi-Target Tracking with a Kalman-Gain CPHD Filter: Simulation and Experimental Validation

Abdullahi Daniyan *

Department of Electrical and Electronic Engineering, Federal University of Technology, Minna, Nigeria.

World Journal of Advanced Engineering Technology and Sciences, 2025, 15(01), 1636-1647

Publication history: Received on 08 March 2025; revised on 17 April 2025; accepted on 19 April 2025

Article DOI: https://doi.org/10.30574/wjaets.2025.15.1.0369

Abstract

We introduce a novel cardinalized implementation of the Kalman-gain-aided particle probability hypothesis density (KG-SMC-PHD) filter, extending it to form the Kalman-Gain Particle Cardinalized Probability Hypothesis Density (KG-SMC-CPHD) filter. This new approach significantly enhances multi-target tracking by combining the particle-based state correction mechanism with the propagation of both the PHD and target cardinality distribution. Unlike conventional particle filters that require a large number of particles for acceptable performance, our method intelligently corrects selected particles during the weight update stage, resulting in a more accurate posterior with substantially fewer particles. Through comprehensive evaluations on both simulated and experimental datasets, the KG-SMC-CPHD filter demonstrates superior robustness and accuracy, particularly in high-clutter environments and nonlinear target dynamics. Notably, it offers improved cardinality estimation and maintains the computational efficiency and performance advantages of its predecessor, the KG-SMC-PHD filter, making it a powerful tool for advanced multi-target tracking applications.

Keywords: Multi-Target Tracking; Particle Filter; Cardinalized PHD; Kalman Gain; Sequential Monte Carlo; Passive Radar

1. Introduction

In multi-target tracking (MTT), the objective is to jointly estimate the states and the number of targets within a surveillance region of interest. This task becomes particularly challenging because the motion of targets can be nonlinear, and targets may enter or exit the scene at random times. Additionally, the measurements received at each time step are often corrupted due to sensor imperfections, false alarms, and missed detections.

To address MTT, several algorithms have been proposed. The most widely used methods include the Joint Probabilistic Data Association (JPDA) filter [1], [2], the Global Nearest Neighbour (GNN) method [1], [3], Multiple Hypothesis Tracking (MHT) [3]-[5], and filters based on Random Finite Sets (RFS) [6]. More recently, message passing algorithms have also been explored [7]-[9]. The GNN, JPDA, and MHT techniques all rely on maintaining multiple instances of single-target filters and require explicit data association followed by single-target filtering [10]. In contrast, RFS-based methods offer the advantage of avoiding data association altogether, focusing instead on estimating the multi-target state through optimal or suboptimal approximations [10]. Message passing introduces a new scalable paradigm for MTT [9].

The Bayesian multi-target filter recursively estimates the multi-target states by propagating the posterior probability density function (pdf) through prediction and update steps. However, exact computation of this multi-target posterior

* Corresponding author: Abdullahi Daniyan.

is intractable, necessitating the use of approximations [6]. By modelling the multi-target states and observations as RFSs and employing the finite set statistics (FISST) framework, tractable solutions can be developed [6].

Among the earliest RFS-based techniques is the Probability Hypothesis Density (PHD) filter, which propagates the first-order moment of an RFS [6]. The Cardinalized PHD (CPHD) filter [11] extends this by jointly propagating the PHD and the cardinality distribution, thus yielding a more accurate estimate of the number of targets. Other notable filters include the multi-target multi-Bernoulli (MeMBer) filter [6] and its cardinality-balanced version, the CMeMBer filter [12]. For further details, readers are referred to standard literature on RFS-based and non-RFS-based MTT methods [10].

The PHD filter [11], [13], has proven effective for tracking multiple time-varying targets without requiring explicit data association. It has been implemented as both a Gaussian Mixture PHD (GM-PHD) filter [14] and a Sequential Monte Carlo or particle PHD (SMC-PHD) filter [15], [16]. The GM-PHD filter assumes a Gaussian mixture model, while the SMC-PHD filter approximates the PHD with weighted particles, making it more suitable for nonlinear and non-Gaussian tracking scenarios. The CPHD filter, implemented both in GM [17], [18] and SMC forms [19], further improves tracking by incorporating the target cardinality distribution.

Although particle-based MTT techniques offer strong performance, they come at the cost of high computational demands due to the large number of particles required. To address this, a Kalman-gain-aided SMC-PHD (KG-SMC-PHD) filter was introduced [20], which improves performance by correcting selected particles using the Kalman gain. This paper extends that concept to the CPHD filter, resulting in the KG-SMC-CPHD filter. This new filter maintains the strengths of the CPHD framework while offering enhanced tracking accuracy and improved cardinality estimation using fewer particles.

The remainder of this paper is structured as follows: Section 2 presents the problem formulation. Section 3 reviews the CPHD filter recursion. Section 4 introduces the proposed KG-SMC-CPHD filter. Simulation and experimental results are discussed in Sections 5 and 6, respectively. Finally, conclusions are drawn in Section 7.

2. Preliminaries

Assume that the multi-target state is given by $\mathbf{X}_k = \{\mathbf{x}_{1,k}, \dots, \mathbf{x}_{T,k}\} \in \mathbb{X}$, where $\mathbb{X}$ denotes the state space. At each time step, a new target may enter the tracking scene, and/or an existing target may leave the scene or evolve to another state.

Let $\mathbf{Z}_k \in \mathbb{Z}$ represent the multi-target observation set at time k, where $\mathbb{Z}$ denotes the observation space. The observation set $\boldsymbol{Z}_k$ comprises measurements generated by actual targets as well as those caused by clutter or false alarms. Due to the uncertainty in both the evolution of targets and the origin of measurements, both $\boldsymbol{X}_{\mathrm{k}}$ and $\boldsymbol{Z}_k$ can be modeled as Random Finite Sets (RFS) [13]. Under the RFS model, this uncertainty is handled using the finite set statistics (FISST) framework [13].

In a recursive Bayesian multi-target filtering framework, the objective is to estimate the posterior pdf, $p_{k|k}(\mathbf{X}_k|\mathbf{Z}_{1:k})$, using prediction and update steps. This estimation is based on the corrupted sets of observations up to and including time step k (i.e., $\mathbf{Z}_{1:K}$: $\mathbf{Z}_1, \mathbf{Z}_2, \dots, \mathbf{Z}_K$). Since exact computation of this posterior is intractable, Mahler [1] proposed propagating only the first-order moment of the posterior, known as the Probability Hypothesis Density (PHD), denoted $D_{k|k}(\mathbf{x}|\mathbf{Z}_{1:k})$. The integral of $D_{k|k}$ over the state space $\mathbb{X}$ yields the expected number of targets [13].

However, as noted in [21], the PHD filter can suffer from a phenomenon known as 'target-death,' where even a single missed detection may cause the erroneous disappearance of a target from the filter's output. This highlights the need for a PHD-type filter that retains the first-order estimation of target states while achieving a higher-order estimation of the number of targets.

To this end, Mahler [11] proposed a method that jointly propagates the PHD $D_{k|k}$ and the cardinality distribution $\rho(n)$, where:

$$\rho(n) = \frac{1}{n!} \int p_{k|k}(\{\mathbf{x}_1, \dots, \mathbf{x}_n\} \mid \mathbf{Z}_{1:k}) d\mathbf{x}_1 \dots d\mathbf{x}_n \dots\dots\dots(1)$$

with $\rho_{k|k}(.|.)$ representing the multi-target posterior probability density. This formulation forms the basis of the Cardinalized PHD (CPHD) filter.

3. The CPHD filter

The Cardinalized Probability Hypothesis Density (CPHD) filter is an extension of the PHD filter $D_{k|k}$. It jointly propagates both the PHD $D_{k|k}$ and the cardinality distribution $\rho_{k|k}(n)$, leading to improved tracking performance at the cost of increased computational complexity [11]. A major source of this complexity arises from the need to compute the elementary symmetric functions (ESFs) during the update step. Nonetheless, methods such as the Newton-Girard formulae have been applied to reduce the implementation burden. In this work, we adopt an alternative CPHD formulation as proposed in [18]. The prediction and update steps of the CPHD filter are detailed below.

3.1. Prediction

The prediction stage involves computing the predicted PHD $D_{k|k-1}$ using the same procedure as in the standard PHD filter [13], along with the predicted cardinality distribution $\rho_{k|k-1}(n)$. The predicted cardinality distribution is obtained by convolving the birth distribution $\rho_{\Gamma,k}$ and the surviving target cardinality distribution $\rho_{S,k|k-1}(i)$:

$$\rho_{k|k-1}(n) = \sum_{i=0}^{n} \rho_{\Gamma,k}(n-i)\rho_{S,k|k-1}(i) \quad \text{..... (2)}$$

The surviving target distribution is given by:

$$\rho_{S,k|k-1}(i) = \sum_{\ell=i}^{\infty} \frac{\ell!}{i!(\ell-i)!} p_S^i (1-p_S)^{\ell-i} \rho_{k-1|k-1}(\ell) \quad \text{..... (3)}$$

where p_S denotes the probability of survival.

3.2. Update

The CPHD update simultaneously refines the predicted PHD $D_{k|k}$ and the predicted cardinality distribution $\rho_{k|k}(n)$ using the measurement set Z_k. The updated cardinality and PHD are given by [11], [18]:

$$\rho_{k|k}(n) = \frac{\Upsilon_k^0[D_{k|k-1};\mathbf{Z}_k](n)\rho_{k|k-1}(n)}{\langle \Upsilon_k^0[D_{k|k-1};\mathbf{Z}_k],\rho_{k|k-1}\rangle} \quad \text{..... (4)}$$

$$D_{k|k}(\mathbf{x}) = \frac{\langle \Upsilon_k^1[D_{k|k-1};\mathbf{Z}_k],\rho_{k|k-1}\rangle(1-p_D(\mathbf{x}))D_{k|k-1}(\mathbf{x})}{\langle \Upsilon_k^0[D_{k|k-1};\mathbf{Z}_k],\rho_{k|k-1}\rangle} + \sum_{\mathbf{z}\in\mathbf{Z}_k} \frac{\langle \Upsilon_k^1[D_{k|k-1};\mathbf{Z}_k\setminus\{\mathbf{z}\}],\rho_{k|k-1}\rangle\psi_{k,\mathbf{z}}(\mathbf{x})D_{k|k-1}(\mathbf{x})}{\langle \Upsilon_k^0[D_{k|k-1};\mathbf{Z}_k],\rho_{k|k-1}\rangle} \quad \text{..... (5)}$$

where $\langle\cdot,\cdot\rangle$ denotes the dot product operator. The sequence $\Upsilon_k^u[D,\mathbf{Z}](n)$ for $u \in \{0,1\}$ is defined as:

$$\Upsilon_k^u[D,\mathbf{Z}](n) = \sum_{i=0}^{min(|\mathbf{Z}|,n)} (|\mathbf{Z}|-i)!\,\rho_{C,k}(|\mathbf{Z}|-i)P_{i+u}^n$$

$$\times \frac{\langle 1-p_{D,k},D\rangle^{n-(i+u)}}{\langle 1,D\rangle^n} e_i\big(\Xi_k(D,\mathbf{Z})\big) \quad \text{..... (6)}$$

where

$$\psi_{k,z}(\mathbf{x}) = \frac{\langle 1,\kappa_k\rangle}{\kappa_k(\mathbf{z})} g_k(\mathbf{z}|\mathbf{x})p_{D,k}(\mathbf{x}) \quad \text{..... (7)}$$

$$\Xi_k(D,\mathbf{Z}) = \langle D,\psi_{k,z}\rangle : \mathbf{z}\in\mathbf{Z} \quad \text{..... (8)}$$

$$P_\ell^n = \frac{n!}{(n-\ell)!} \quad \text{..... (9)}$$

The term $P_\ell^n = \frac{n!}{(n-\ell)!}$ is the number of permutations. The ESF $e_i(\cdot)$ represents the elementary symmetric function of order i, computed over $\Xi_k(D,\mathbf{Z})$.

The CPHD recursion described above has two main implementations: the Gaussian Mixture CPHD (GM-CPHD) filter [18], which assumes linear-Gaussian dynamics, and the particle-based CPHD filter [19], which is well-suited to nonlinear and non-Gaussian scenarios. The enhancements proposed in this paper pertain to the particle-based implementation.

4. The Kalman-Gain-Aided SMC-CPHD Filter

The KG-SMC-CPHD filter seeks to achieve a more accurate posterior by applying particle state correction during the update stage of the standard SMC-CPHD filter. This is accomplished using the Kalman gain technique in conjunction with a validation threshold. The validation threshold is used to identify promising particles associated with a target and relocate them to regions of higher likelihood in order to obtain a more accurate posterior. We first present the prediction stage of the KG-SMC-CPHD filter, followed by the update stage.

4.1. Prediction

The prediction stage of the KG-SMC-CPHD filter is similar to that of the standard SMC-CPHD filter (see e.g. [19]). Assume that at time *k–1*, the cardinality distribution is $\rho_{k-1|k-1}(n)$, and that the PHD $D_{k-1|k-1}$is given by a set of particles with associated weights $\{\mathbf{x}_{k-1}^{j}, w_{k-1}^{j}\}_{j=1}^{L_{k-1}}$

Predict the cardinality distribution according to the CPHD recursion (2). Predict the PHD $D_{k|k-1}$ by drawing L_k and J_k samples with associated weights for surviving and newborn targets, respectively, from two proposal distributions:

$$\mathbf{x}_{k|k-1}^{j} \approx \begin{cases} q_k(\cdot \mid \mathbf{x}_{k-1}^{j}, \mathbf{Z}_k), & j = 1, \dots, L_k \\ p_k(\cdot \mid \mathbf{Z}_k), & j = L_k + 1, \dots, \mathcal{L}_k \end{cases} \quad \text{..... (10)}$$

$$w_{k|k-1}^{j} = \begin{cases} \frac{p_S(\mathbf{x}_{k-1}) f_{k|k-1}(\mathbf{x}_k, \mathbf{x}_{k-1})}{q_k(\mathbf{x}_{k|k-1} \mid \mathbf{x}_{k-1}^{j}, \mathbf{Z}_k)} w_{k-1}^{j}, & j = 1, \dots, L_k \\ \frac{\gamma_k(\mathbf{x}_k^{j})}{J_k p_k(\mathbf{x}_{k|k-1} \mid \mathbf{Z}_k)}, & j = L_k + 1, \dots, \mathcal{L}_k \end{cases}$$

The predicted PHD is given by:

$$D_{k|k-1}(\mathbf{x} \mid \mathbf{Z}_{k-1}) = \sum_{j=1}^{\mathcal{L}_k} w_{k|k-1}^{j} \delta(\mathbf{x}_{k|k-1}^{j}) \quad \text{..... (11)}$$

Here, $q_k(\cdot|\cdot)$ and $p_k(\cdot|\cdot)$ denote proposal distributions for surviving and newborn targets, respectively. $p_S(\cdot)$ is the probability of survival, $\mathcal{L}_k = L_k + J_k$, $\gamma_k(\cdot)$is the PHD of spontaneous birth, and $f_{k|k-1}(\cdot,\cdot)$ is the single-target motion model.

4.2. Update

Our proposed enhancement is applied during the update stage. The PHD is first updated using the CPHD equations (5), followed by updating the cardinality distribution (4).

We identify and select predicted particles for state correction. A predicted particle $\mathbf{x}_{k|k-1}^{j}$ is selected for correction if, for each $\mathbf{z}_k \in \mathbf{Z}_k$, the following condition is satisfied:

$$g(\dot{\mathbf{z}}_k^{n} \mid \mathbf{x}_{k|k-1}^{j}) \geq \tau, \text{ for } j = 1, \dots, \mathcal{L}_k \quad \text{.....(12)}$$

Here, *g(·|·)* is the measurement likelihood function, and τ is a threshold inversely proportional to the total number of samples per persistent target [20]. The term $\dot{\mathbf{z}}_k^{n}$ represents a clutter-free measurement, defined as:

$$\dot{\mathbf{Z}}_k = \bigcup_{n=1}^{n_s} \{\dot{\mathbf{z}}_k^{n}\}, \quad \text{..... (13)}$$

where $\dot{\mathbf{Z}}_k \subset \mathbf{Z}_k$and $n_s = \left|\dot{\mathbf{Z}}_k\right|$.

Each particle satisfying the above condition in (12) is a candidate for correction. The corrected state is computed as:

$$\mathbf{x}_k^j = \mathbf{x}_{k|k-1}^j + \mathbf{K}_k(\dot{\mathbf{z}}_k^n - h(\mathbf{x}_{k|k-1}^j)) \quad \text{..... (14)}$$

$$\mathbf{K}_k = \mathbf{M}_{k-1}\mathbf{H}_k^T\mathbf{P}_k^{-1} \quad \text{..... (15)}$$

$$\mathbf{P}_k^{-1} = \mathbf{R}_k + \mathbf{H}_k\mathbf{M}_{k-1}\mathbf{H}_k^T \quad \text{..... (16)}$$

$$\mathbf{M}_k = \mathbf{M}_{k-1} - \mathbf{K}_k\mathbf{H}_k\mathbf{M}_{k-1} \quad \text{..... (17)}$$

where $\mathbf{K}_k$ is the Kalman gain, $\mathbf{H}$ is the measurement transformation matrix, $h(\cdot)$ is the measurement projection function, $\mathbf{R}$ is the measurement noise covariance, $\mathbf{M}$ is the state estimation covariance, and $\mathbf{P}$ is the innovation covariance matrix.

Following state correction, the CPHD update sequence is computed. Then the updated cardinality distribution $\rho_{k|k}(n)$ using (4) and particle weights $w_{k|k}^j$ are determined according to (5). The estimated number of targets is given by:

$$N_k = \sum_{j=1}^{\mathcal{L}_k} w_{k|k}^j \quad \text{..... (18)}$$

and the updated PHD is represented as:

$$D_{k|k}(\mathbf{x}_k \mid \mathbf{Z}_k) = \sum_{j=1}^{\mathcal{L}_k} w_k^j \delta(\mathbf{x}_k^j) \quad \text{..... (19)}$$

5. Simulation results and discussion

In this section, we compare the performance of the KG-SMC-CPHD filter with the SMC implementation of the CPHD filter from [11, 18], which we refer to as the standard SMC-CPHD filter, using simulated data.

We assume a sensor $[x_s, y_s]^T$ located at the origin of the x-y Cartesian coordinate system that generates noisy range-bearing measurements of the targets, including false alarms. Target-originated measurements follow a nonlinear model:

$$\mathbf{z}_k = \begin{bmatrix} r_k \\ \theta_k \end{bmatrix} + \mathbf{n}_k \quad \text{..... (20)}$$

with

$$r_k = \left\| \begin{bmatrix} 1 & 0 & 0 & 0 \\ 0 & 1 & 0 & 0 \end{bmatrix} \mathbf{x}_k - \begin{bmatrix} x_s \\ y_s \end{bmatrix} \right\|, \theta_k = \arctan\left(\frac{[0\ 1\ 0\ 0]\mathbf{x}_k + y_s}{[1\ 0\ 0\ 0]\mathbf{x}_k + x_s}\right) \quad \text{..... (21)}$$

include measurement noise with a zero-mean Gaussian distribution. The noise has a covariance matrix $\mathbf{R} = \text{diag}([\sigma_r^2, \sigma_\theta^2])$, where σ_r = 9 m and σ_θ = 0.45 radians. Clutter is modeled as a Poisson point process with an average of λ = 20 clutter points per scan and is uniformly distributed.

A total of 8 targets enter and exit the tracking scene with multiple crossings. A plot of the ground truth showing the true trajectories, start, and end positions is presented in Fig. 1. The target dynamics follow a nearly constant turn model:

$$\mathbf{x}_k = \begin{bmatrix} 1 & 0 & \frac{sin(\omega\Delta t)}{\omega} & -\frac{1-cos(\omega\Delta t)}{\omega} \\ 0 & 1 & \frac{1-cos(\omega\Delta t)}{\omega} & \frac{sin(\omega\Delta t)}{\omega} \\ 0 & 0 & cos(\omega\Delta t) & -sin(\omega\Delta t) \\ 0 & 0 & sin(\omega\Delta t) & cos(\omega\Delta t) \end{bmatrix} \mathbf{x}_{k-1} + \begin{bmatrix} \frac{\Delta t^2}{2} & 0 \\ 0 & \frac{\Delta t^2}{2} \\ \Delta t & 0 \\ 0 & \Delta t \end{bmatrix} \mathbf{v}_k \quad \text{..... (22)}$$

where $\omega_k = \omega_{k-1} + \Delta t u_{k-1}$, $\Delta t = 1$ s. The state vector is $\mathbf{x}_k = [x_k, y_k, x_k, y_k, \omega_k]^T$. Noise terms: $\mathbf{v}_k \sim \mathcal{N}(0, \sigma_v^2 I)$, $u_k \sim \mathcal{N}(0, \sigma_u^2)$ with $\sigma_v = 10$ m/s^2, $\sigma_u = \pi/180$ rad/s. The variable η denotes the number of particles used per existing target.

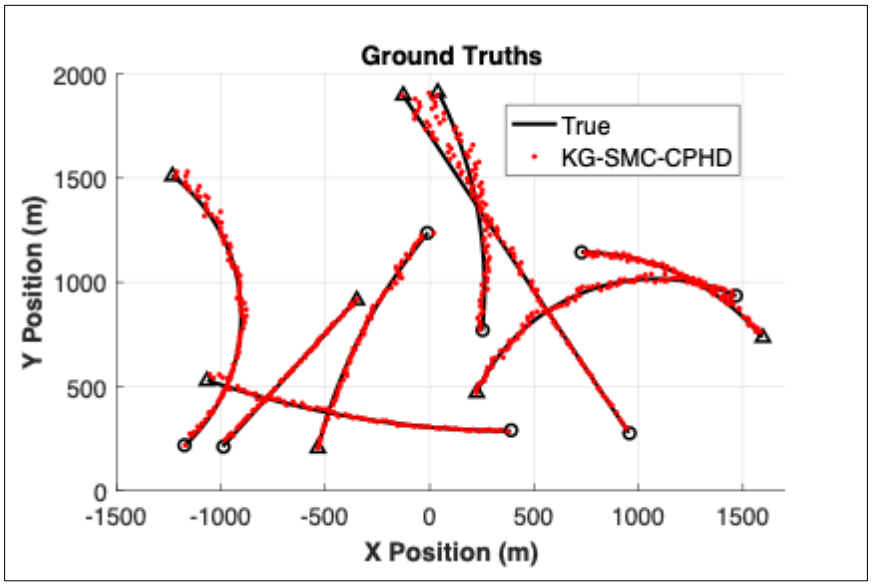

Figure 1 Plots showing the KG-SMC-CPHD filter estimates superimposed on the true target trajectories. The true start/end positions of the targets are indicated by ◯/△.

Figure 1 shows a single Monte Carlo (MC) run with the estimated trajectories superimposed on the true tracks. The KG-SMC-CPHD filter is able to track all targets, even during multiple crossings. Figure 2 presents x- and y-coordinates over time, showing successful identification of target birth and death events. With η = 500, the filter accurately tracks all targets and resolves closely spaced targets even under nonlinear dynamics and high clutter.

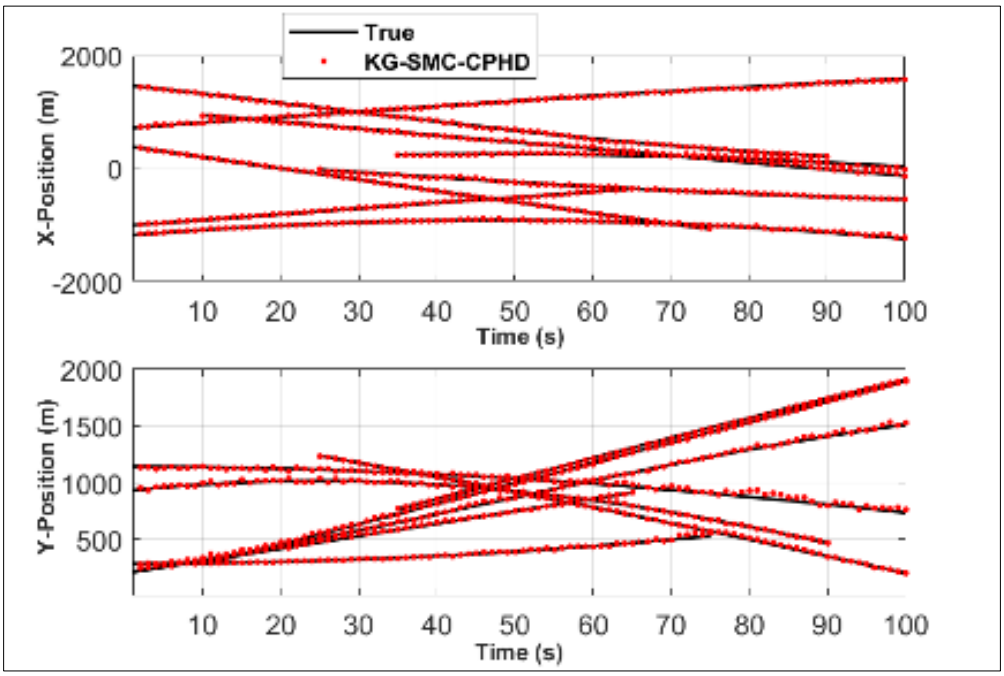

Figure 2 x and y components vs time of the true target trajectories and the KG-SMC-CPHD filter estimates

Figures 3 and 4 compare cardinality statistics of the KG-SMC-PHD filter [20] and the KG-SMC-CPHD filter. The KG-SMC-PHD filter shows high variance, while the KG-SMC-CPHD filter yields a lower standard deviation due to joint propagation of the PHD and cardinality distribution.

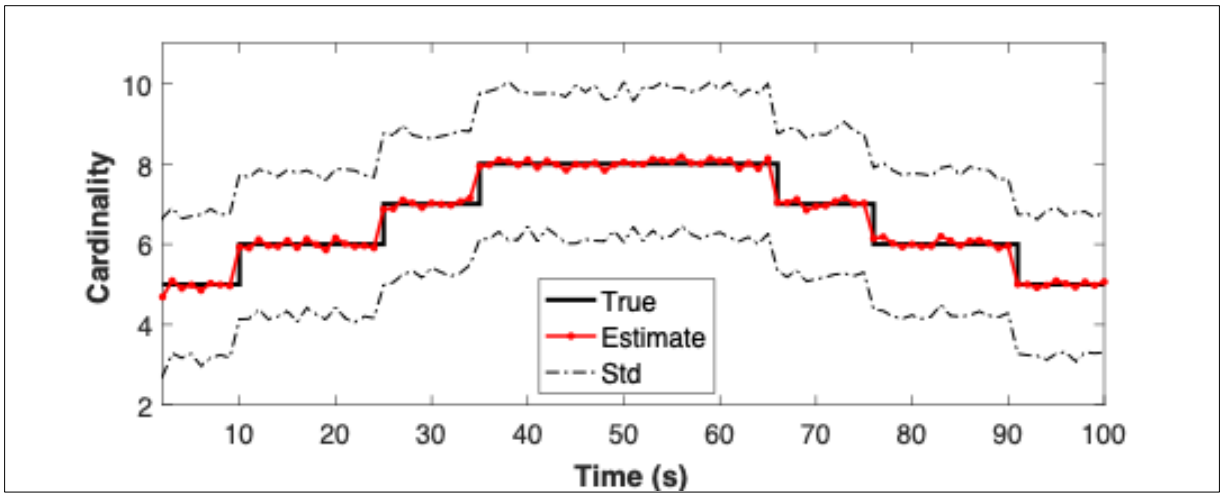

Figure 3 KG-SMC-PHD filter: True and estimated cardinality statistics vs time averaged over 100 MC trials. The red-dot-line denote the mean cardinality estimates to one decimal place and Std is the standard deviation

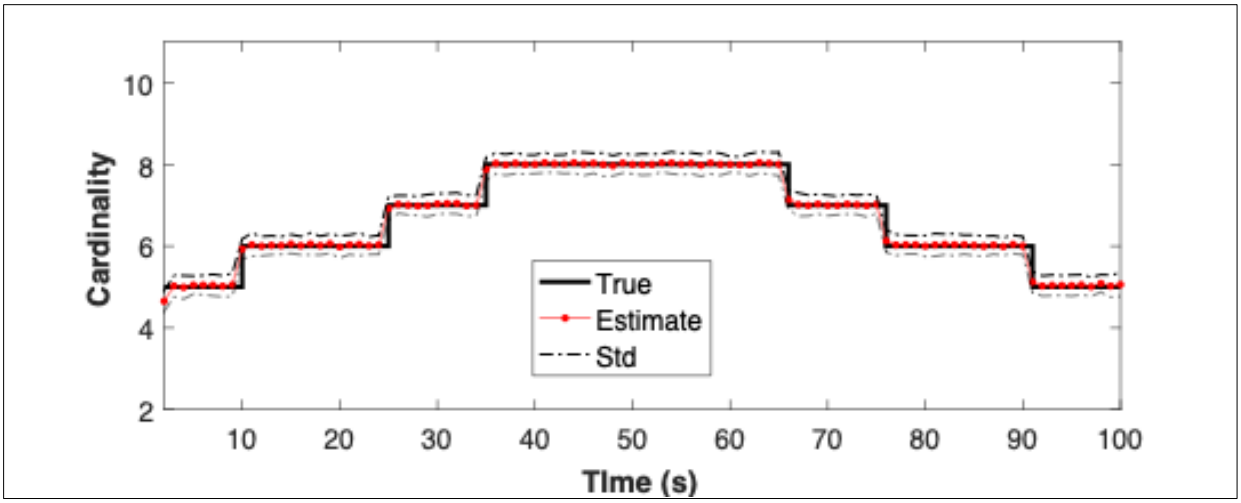

Figure 4 KG-SMC-CPHD filter: True and estimated cardinality statistics vs time averaged over 100 MC trials. The red-dot-line denote the mean cardinality estimates to one decimal place and Std is the standard deviation

Table 1 Filter performance in terms of number of particles, OSPA distance and CT for λ= 20. Different values for number of particles per existing target (η) are considered

Filter	Particles	OSPA (m)	ET (s)
SMC-CPHD	50	57.00	1.1
	100	41.41	1.5
	500	32.13	4.7
	1000	28.49	8.4
KG-SMC-CPHD	50	38.36	2.0
	100	33.77	2.4
	500	20.79	5.3
	1000	15.04	9.0

To compare estimation accuracy, we use the Optimal Subpattern Assignment (OSPA) metric [22] and execution time (ET). Table 1 presents performance metrics averaged over 100 MC runs for different values of η. As η increases, both filters show reduced OSPA distances, indicating improved accuracy. However, ET for the KG-SMC-CPHD filter is higher due to the additional state correction step. Despite this, the KG-SMC-CPHD filter achieves better accuracy with fewer particles, making it more efficient overall.

Figure 4 shows the OSPA distance for c = 100 and p = 1, comparing the KG-SMC-CPHD filter and the SMC-CPHD filter using the same targets. The proposed filter consistently achieves lower OSPA values. Figure 6 shows that execution time increases with the number of particles, as expected. Interestingly, for η < 1000, the KG-SMC-CPHD filter has slightly higher ET due to correction overhead. However, beyond this threshold, its ET becomes competitive, indicating that the computational cost of particle correction is marginal for larger η values.

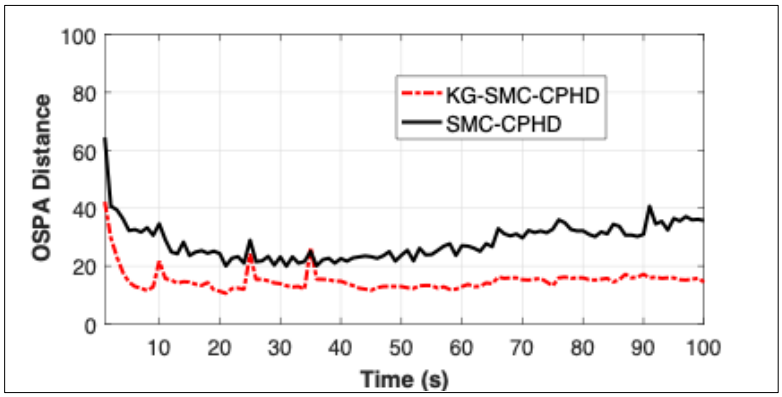

Figure 5 OSPA distance measure against tracking time. Results shown are averaged over 100 MC trials

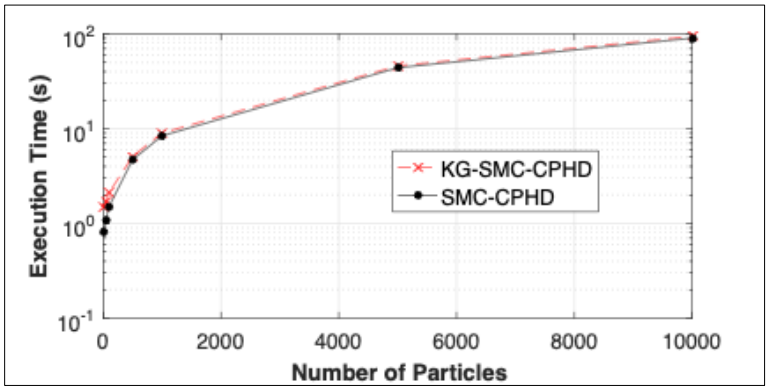

Figure 6 Execution time against number of particles per target. Results shown are averaged over 100 MC trials

6. Experimental results

We compare the performance of the KG-SMC-CPHD filter with that of the standard SMC-CPHD filter using real measurement data obtained in a passive coherent localization (PCL) experiment. The goal is to track multiple aircraft using noisy bi-static range and radial velocity measurements. The PCL data used here is the same as that in [23]. The true locations of the aircraft were obtained using data reported in [24].

6.1. Experimental Set-up

The transmitter of opportunity was an FM station located approximately 6.5 km from the receiver, operating at a center frequency of 106 MHz. The passive receiver consisted of a National Instruments USRP-2950R software-defined radio platform connected to two FM antennas—one for the surveillance channel and the other for the reference channel. The USRP was interfaced with LabVIEW to record raw I/Q data over 732 seconds. Post-processing generated bi-static range and radial velocity measurements of aircraft within the surveillance region.

The radar had a bi-static radial velocity resolution of 1.4 m/s and a bi-static range resolution of 937.5 m. The detection range extended up to 48 km, with a minimum altitude of 100 m. Processed data were stored as intensity maps with bi-static range on the x-axis and radial velocity on the y-axis. Constant false alarm rate (CFAR) detection was applied using a false alarm probability of $P_{FA} = 1 \times 10^{-4}$, resulting in an estimated clutter rate of $\lambda = 15$ clutter points per time step. Figures 5a and 5b show sample intensity maps before and after applying CFAR. Centroiding was performed to extract single-point detections before tracking.

6.2. Filter Parameters

A constant velocity dynamic model was used for tracking. The state model is: $\hat{\mathbf{x}}_k = \hat{\mathbf{F}}\hat{\mathbf{x}}_{k-1} + \hat{\mathbf{v}}_k$

with

$$\hat{\mathbf{F}} = \begin{bmatrix} 1 & \Delta t \\ 0 & 1 \end{bmatrix}, \hat{\mathbf{Q}} = \begin{bmatrix} \frac{\Delta t^4}{4} & \frac{\Delta t^3}{2} \\ \frac{\Delta t^3}{2} & \Delta t^2 \end{bmatrix}$$

$$\hat{\mathbf{x}}_k = [\hat{r}_k, v_k]^T, \ \hat{\mathbf{v}}_k \sim \mathcal{N}(0, \sigma^2 \hat{\mathbf{Q}}), \sigma = 0.02 \text{ km/s}^2$$

where Δt = 1 s.

The measurement model is:

$$\hat{\mathbf{z}}_k = \mathbf{H}\begin{bmatrix} \hat{r}_k \\ v_k \end{bmatrix} + \hat{\mathbf{n}}_k \text{with } \mathbf{H} = \text{diag}([1,1]),$$

$$\hat{\mathbf{n}}_k \sim \mathcal{N}(0, \hat{\mathbf{R}}), \hat{\mathbf{R}} = \text{diag}([\sigma_{\hat{r}}^2, \sigma_v^2])$$

with $\sigma_{\hat{r}} = 30$ m and $\sigma_v = 4.5$ m/s. An adaptive birth model was used for new targets.

A total of six aircraft entered and exited the tracking region during the experiment. Figures 6a and 6b show results from a sample run using the KG-SMC-CPHD filter. η was set to 1000 for existing tracks and η/5 for new ones. In Figure 6a, black lines represent true aircraft paths while red dots represent filter estimates. The filter successfully tracked all aircraft, including those that passed directly over the radar setup. These aircraft displayed characteristic 'C'-shaped paths—positive radial velocity when approaching, zero when closest, and negative when receding.

Figure 6b shows the cardinality estimation over time, averaged over 100 Monte Carlo (MC) runs. The filter closely matches the ground truth, indicating robust estimation of the number of targets throughout the experiment.

Table 2 Filter performance in terms of number of particles, OSPA distance and ET averaged over 100 MC runs

Filter		OSPA (m)	ET (s)
SMC-CPHD	50	790.51	3.71
	100	759.70	7.21
	500	669.74	10.91
	1000	613.53	15.60
KG-SMC-CPHD	50	432.12	4.02
	100	417.30	8.85
	500	405.77	10.64
	1000	389.16	14.22

Table 2 summarizes the performance comparison of both filters in terms of number of particles (η), average OSPA distance, and execution time (ET). The KG-SMC-CPHD filter achieved an average OSPA of 432.12 m with just 50 particles per target, outperforming the SMC-CPHD filter even at η = 1000. While the SMC-CPHD filter is initially faster for lower η, the KG-SMC-CPHD filter becomes more efficient for η ≥ 500. This is because the CPHD filter requires computation of elementary symmetric functions over all particles, whereas our method performs these only on selected particles.

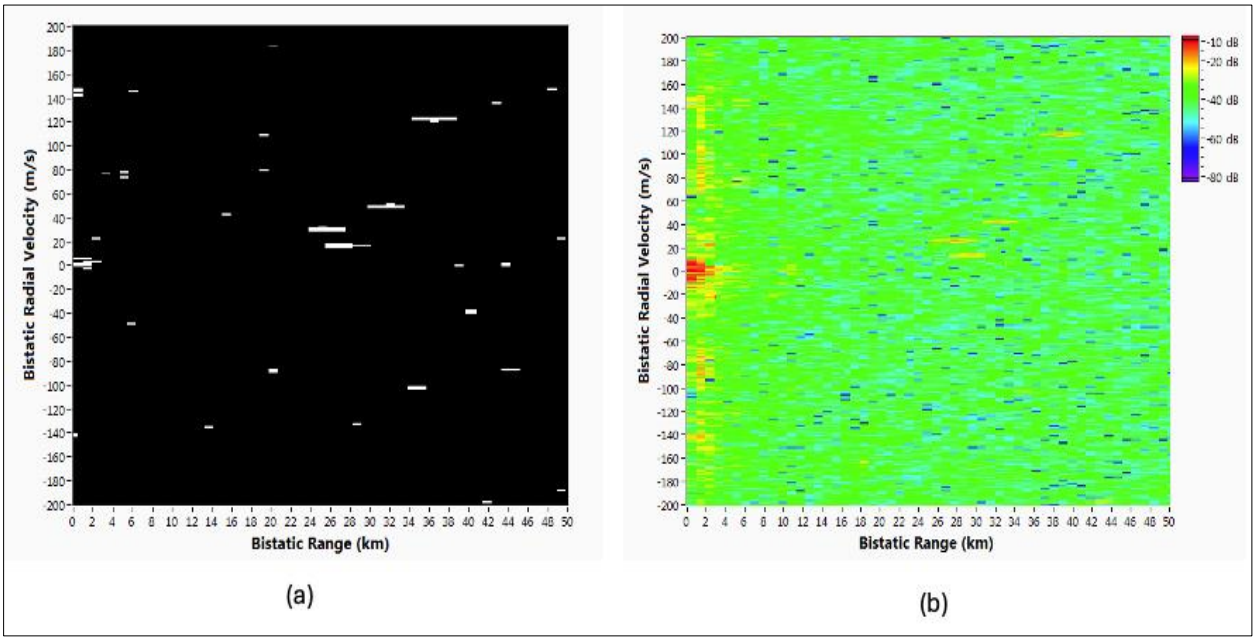

Figure 7 Bi-static radial velocity vs bi-static range map obtained from the passive radar set-up at time = 109s. (a) Bi-static radial velocity vs bi-static range map after CFAR. (b) Bi-static radial velocity vs bi-static range intensity map before CFAR

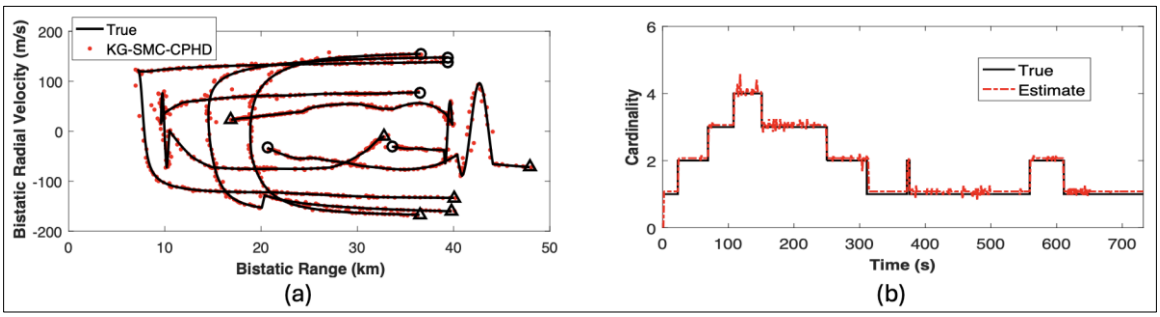

Figure 8 (a) Plot showing the KG-SMC-CPHD filter estimates (red dots) for a single MC run superimposed on true bi-static radial velocity vs bi-static range of various aeroplanes (solid black line) for the whole duration of the experiment. Start/End for each target are shown with ◯/△. (b) True and KG-SMC-CPHD filter cardinality estimates of flights vs time averaged over 100 MC runs

7. Conclusion

This paper has presented the Kalman-Gain-aided Sequential Monte Carlo Cardinalized Probability Hypothesis Density (KG-SMC-CPHD) filter—an enhanced multi-target tracking algorithm that significantly advances the performance of particle-based CPHD filtering. By integrating a selective particle state correction strategy based on the Kalman gain, the proposed method achieves high-precision tracking with a reduced number of particles. Simulation results reveal that the KG-SMC-CPHD filter outperforms both the standard SMC-CPHD and the KG-SMC-PHD filters, particularly in terms of cardinality estimation accuracy, robustness in cluttered environments, and OSPA distance metrics. Furthermore, real-world experimental validation using passive coherent localization data underscores the filter's practical utility and

efficiency. Overall, the KG-SMC-CPHD filter delivers a compelling balance between accuracy and computational efficiency, making it a strong candidate for deployment in complex, real-time tracking scenarios involving multiple targets and uncertain dynamics.

Compliance with ethical standards

Disclosure of conflict of interest

No conflict of interest to be disclosed.

References

[1] Y. Bar-Shalom, P. K. Willett, and X. Tian, Tracking and data fusion. YBS publishing, 2011.

[2] S. Challa, Fundamentals of object tracking. Cambridge University Press, 2011.

[3] S. Blackman and R. Popoli, Design and Analysis of Modern Tracking Systems, ser. Artech House radar library. Artech House, 1999.

[4] S. S. Blackman, "Multiple Hypothesis Tracking for Multiple Target Tracking," IEEE Aerospace and Electronic Systems Magazine, vol. 19, no. 1, pp. 5–18, Jan 2004.

[5] D. Reid, "An algorithm for tracking multiple targets," IEEE Transactions on Automatic Control, vol. 24, no. 6, pp. 843–854, Dec 1979.

[6] R. P. Mahler, Statistical Multisource-Multitarget Information Fusion. Artech House, Inc., 2007.

[7] F. Meyer, P. Braca, P. Willett, and F. Hlawatsch, "A scalable algorithm for tracking an unknown number of targets using multiple sensors," IEEE Transactions on Signal Processing, vol. 65, no. 13, pp. 3478–3493, July 2017.

[8] J. Williams and R. Lau, "Approximate evaluation of marginal association probabilities with belief propagation," IEEE Transactions on Aerospace and Electronic Systems, vol. 50, no. 4, pp. 2942–2959, 2014.

[9] F. Meyer, T. Kropfreiter, J. L. Williams, R. Lau, F. Hlawatsch, P. Braca, and M. Z. Win, "Message passing algorithms for scalable multitarget tracking," Proceedings of the IEEE, vol. 106, no. 2, pp. 221–259, Feb 2018.

[10] B.-N. Vo, M. Mallick, Y. Bar-Shalom, S. Coraluppi, R. Osborne III, R. Mahler, and B.-T. Vo, "Multitarget Tracking," Wiley Encyclopedia of Electrical and Electronics Engineering, Sept 2015.

[11] R. Mahler, "PHD filters of Higher Order in Target Number," IEEE Transactions on Aerospace and Electronic Systems, vol. 43, no. 4, pp. 1523–1543, October 2007.

[12] B.-T. Vo, B.-N. Vo, and A. Cantoni, "The Cardinality Balanced Multi-Target Multi-Bernoulli Filter and Its Implementations," IEEE Transactions on Signal Processing, vol. 57, no. 2, pp. 409–423, 2009.

[13] R. P. S. Mahler, "Multitarget Bayes Filtering via First-Order Multitarget Moments," IEEE Transactions on Aerospace and Electronic Systems, vol. 39, no. 4, pp. 1152–1178, Oct 2003.

[14] B.-N. Vo and W.-K. Ma, "The Gaussian Mixture Probability Hypothesis Density Filter," IEEE Transactions on Signal Processing, vol. 54, no. 11, pp. 4091–4104, 2006.

[15] B.-N. Vo, S. Singh, and A. Doucet, "Random Finite Sets and Sequential Monte Carlo Methods in Multi-Target Tracking," in Proceedings of the International Radar Conference, 2003, pp. 486–491.

[16] B.-N. Vo, S. Singh, and A. Doucet, "Sequential Monte Carlo Methods for Multitarget Filtering with Random Finite Sets," IEEE Transactions on Aerospace and Electronic Systems, vol. 41, no. 4, pp. 1224–1245, Oct 2005.

[17] B.-T. Vo, B.-N. Vo, and A. Cantoni, "The Cardinalized Probability Hypothesis Density Filter for Linear Gaussian Multi-Target Models," in 2006 40th Annual Conference on Information Sciences and Systems, 2006, pp. 681–686.

[18] B. T. Vo, B. N. Vo, and A. Cantoni, "Analytic Implementations of the Cardinalized Probability Hypothesis Density Filter," IEEE Transactions on Signal Processing, vol. 55, no. 7, pp. 3553–3567, July 2007.

[19] B. Ristic, D. Clark, B. N. Vo, and B. T. Vo, "Adaptive Target Birth Intensity for PHD and CPHD Filters," IEEE Transactions on Aerospace and Electronic Systems, vol. 48, no. 2, pp. 1656–1668, April 2012.

[20] A. Daniyan, Y. Gong, S. Lambotharan, P. Feng, and J. Chambers, "Kalman-Gain Aided Particle PHD Filter for Multitarget Tracking," IEEE Transactions on Aerospace and Electronic Systems, vol. 53, no. 5, pp. 2251–2265, Oct 2017.

[21] O. Erdinc, P. Willett, and Y. Bar-Shalom, "A Physical-Space Approach for the Probability Hypothesis Density and Cardinalized Probability Hypothesis Density Filters," in Defense and Security Symposium. International Society for Optics and Photonics, 2006, pp. 623619–623619.

[22] D. Schuhmacher, B. T. Vo, and B. N. Vo, "A Consistent Metric for Performance Evaluation of Multi-Object Filters," IEEE Transactions on Signal Processing, vol. 56, no. 8, pp. 3447–3457, Aug 2008.

[23] A. Daniyan, A. Aldowesh, Y. Gong, and S. Lambotharan, "Data Association using Game Theory for Multi-target Tracking in Passive Bistatic Radar," 2017 IEEE Radar Conference (RadarConf), 2017, pp. 0042–0046.

[24] Flightradar24. (2016) Flightradar24.com - live flight tracker! [Online]. Available: https://www.flightradar24.com